ELSEVIER

Chemical Engineering Journal 130 (2007) 125–133

Chemical Engineering Journal

www.elsevier.com/locate/cej

The investigation of gas holdup distribution in a two-phase bubble column using ultrasonic computed tomography

Muhammad Dani Supardan [a], Yoshifumi Masuda [b], Akinori Maezawa [b], Shigeo Uchida [b,*]

[a] *Department of Chemical Engineering, Syiah Kuala University, Darussalam, Banda Aceh 23111, Indonesia*
[b] *Department of Materials Science and Chemical Engineering, Shizuoka University, 3-5-1 Johoku, Hamamatsu 432-8561, Japan*

Abstract

In this study, time-averaged gas holdup distributions were investigated in a 16 cm diameter bubble column for two-phase dispersed system of air–water and air–glycerol solution of 10 wt% by using ultrasonic computed tomography (UCT). A quantitative result of UCT – as a coupling of the ultrasonic transmission method and the iterative filtered backprojection (IFBP) image reconstruction technique – is presented. The UCT results are in a good agreement with those by the bed expansion method. A higher gas holdup in the air–glycerol 10 wt% solution than in the air–water system was observed. The distribution of gas holdup in the column with an attached baffle is also investigated by UCT.

Keywords: Bubble column; Gas holdup; Iterative filtered backprojection; Ultrasonic computed tomography

1. Introduction

Gas holdup is a very important parameter for mass transfer operation in bubble columns. The average gas holdup is a global parameter and it is important in deciding the size of reactor. The radial gas holdup distributions will give local gas concentration, and help understanding the flow pattern. The development and the application of non-intrusive and non-invasive measuring technique capable of investigating gas holdup distributions will greatly facilitate current efforts to predict and improve reactor performance. Neal and Bankoff [1] first made measurement of radial gas holdup distribution in the two-phase flow using an electrical resistivity probe. Since then, many measurements using different techniques have been reported. Various conventional measuring techniques such as the hot wire probe, electro-resistivity probe, optical fiber probe as well as pressure tap and shutter plate, have been devised. However, these are not suitable because the measurement themselves interfere the motion of bubbles, and consequently vary the hydrodynamics of the system.

In recent years, the applications of tomographic techniques as a robust non-invasive tool for direct analysis of the characteristics of multiphase flows have increased. The application of process tomography for investigating gas holdup distributions in a bubble column is the major subject of many researches [2–6]. Electrical resistance tomography and gamma and X-ray tomography have been used for imaging gas holdup spatial distribution. Besides inherent limitation of ultrasonic technique, the tomography using ultrasound wave has recently been paid considerable attention. Hoyle and Xu [7] reviewed the application of ultrasonic sensors in the process tomography. Xu et al. [8] developed a transmission-mode ultrasonic computed tomography (UCT) system involving a fan-shape beam scanning geometry and a fast binary backprojection filtering algorithm. The relatively slow speed of sound as one of major inherent UCT limitations is proposed to be offset through the use of a novel spectral analysis [9]. Warsito et al. [10] proposed an UCT technique for investigating the cross-sectional distribution of the gas and solid holdups in a slurry bubble column. Utomo et al. [11] have also reported the flow structure in a slurry bubble column containing fine particle (TiO_2) using UCT improved with an interpolating technique.

In the process tomography, the distribution of local measurement property is calculated from the measured values after the measurements have been conducted. This is done by the so-called image reconstruction technique. The choice of the image reconstruction technique is one of crucial steps as it determines the quality of the image to be produced. For linear tomographies such as the X-ray computed tomography, the gamma ray

* Corresponding author. Tel.: +81 53 478 1170; fax: +81 53 478 1170.
E-mail address: tcsuchi@ipc.shizuoka.ac.jp (S. Uchida).

1385-8947/$ – see front matter © 2007 Published by Elsevier B.V.
doi:10.1016/j.cej.2006.08.035

Nomenclature

d_b	radius of bubble (cm)
g	acceleration due to gravity (cm/s^2)
H	UCT measurement position above the distributor (cm)
I	ultrasonic intensity in a dispersed system (V)
I_0	ultrasonic intensity in liquid (V)
k	wave number (cm^{-1})
L	ultrasound transmission path length (cm)
$p(s, \theta)$	projection data
r_e	equivalent radius of bubble (cm)
U_g	superficial gas velocity (cm/s)
V_∞	terminal velocity of bubble (cm/s)
X_G	coefficient defined in Eq. (2)

Greek letters

α	attenuation coefficient (cm^{-1})
δ	gain factor
ε_G	local gas holdup
Φ	scattering coefficient
λ	ultrasound wavelength (cm)
μ	dynamic viscosity of fluid (mPa s)
θ	projection angle (rad)
ρ	density of fluid (kg/m^3)
σ	surface tension of fluid (mN/m)

tomography and the ultrasonic tomography, a well-known filtered backprojection (FBP) technique has often been used in the tomographic reconstruction. In fact, FBP requires a large number of integral measurement data to obtain a reliable accuracy and the results are still rather sensitive to noise. The noise arises as a result of unmodelled or unmodellable processes going on in the production and capture of the real signal. It is not a part of the ideal signal and may be caused by a wide range of sources, such as variations in the detector sensitivity, environmental variations, the discrete nature of radiation, transmission or quantization errors, etc. Noisy imaging problems arise in a variety of context and often yield unacceptable results. It may degrade further analysis and interpretation of the data. Recently, Utomo et al. [11] used iterative filtered backprojection (IFBP) technique to analyze distributions of gas and solid in slurry bubble column using UCT. They showed that IFBP outperformed FBP technique to reconstruct the model images. In the iterative procedure, the property distribution will be revised according to the sum of all the errors between the measured data and the estimated value. It will diminish the effect of noise contained in the measured data.

This study is a continuation of our earlier studies [10,11], which focused the application of UCT on slurry bubble column. The main objective of the present study is to show further the capability of UCT for predicting gas holdup in a bubble column. UCT with IFBP reconstruction technique was used to investigate the gas holdup distribution in a two-phase bubble column of air–water and air–glycerol 10 wt% systems. To provide the attenuation and the local gas holdup relationship, a different approach with our earlier studies is implemented by conducting preliminary experiments of ultrasound in rectangular bubble column. The capability of UCT to investigate the gas holdup distribution in a bubble column with an attached baffle is also presented.

2. Experimental

2.1. Preliminary experiments in rectangular bubble column

Warsito et al. [10] and Utomo et al. [11] reported that both gas holdup and solid holdup could be obtained simultaneously by applying two ultrasound parameters of the attenuation energy and the time difference. Based on the experimental data, they derived correlations between the phase holdup and the ultrasound parameters. In this study, however, only the attenuation energy of ultrasound is used to obtain the gas holdup. Hence, the determination of slow speed of sound as inherent UCT limitation is not required.

The first problem to be solved is how to establish the relationship between the attenuation energy as an ultrasound parameter and the local gas holdup. The energy attenuation of an ultrasound wave passing through a medium is generally described by

$$-\ln\left(\frac{I}{I_0}\right) = \alpha L \tag{1}$$

where I is the ultrasonic intensity transmitted in the dispersed system and I_0 is the ultrasonic intensity transmitted in the liquid phase only. For a two-phase system, Warsito et al. [10] showed that the attenuation coefficient, α for gas bubbles could be expressed as $X_G\varepsilon_G$, and therefore Eq. (1) can be written as follows

$$-\ln\left(\frac{I}{I_0}\right) = X_G\varepsilon_G L \tag{2}$$

where the parameter X_G can be obtained from the experiments. Generally, X_G was dependent on the ultrasonic frequency, bubble diameter and physical properties of gas/liquid. Stolojanu and Prakash [12] also introduced a correlation similar to Eq. (2):

$$-\ln\left(\frac{I}{I_0}\right) = \left(\frac{3k}{8\Phi}\right)\varepsilon_G L \tag{3}$$

where k is the wave number of the ultrasonic wave and Φ is the scattering coefficient. Both Eqs. (2) and (3) show that the attenuation energy increases as the gas holdup increases.

A preliminary experiment with a rectangular bubble column was performed to provide a relationship between the attenuation energy and the local gas holdup, ε_G. The column was made of methylmethaacrylate, 125 cm in height, 20 cm in width and 2 cm in depth. The experimental setup is presented in Fig. 1. Tap water and glycerol solution with concentration of 10 wt% were used as the liquid phase. The physical properties of the liquids are shown in Table 1. The density, the viscosity and the surface tension were measured with use of picnometer, capillary viscometer and du Nouy-type surface tensiometer, respectively,

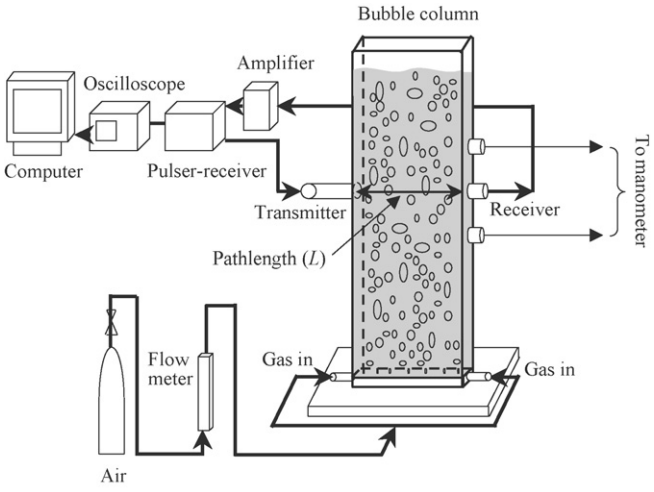

Fig. 1. Rectangular bubble column experimental setup.

at the temperature of 25 °C. Air was used as the gas phase. The experiments were conducted batchwise with respect to the liquid phase.

The ultrasound frequency used in the measurement was 2 MHz. The ultrasonic measurement may produce erroneous results if not used properly, since diffraction and/or reflection effects may dominate, depending upon the properties of the object being interrogated and the operating frequency of the ultrasound wave. In a bubbly air–water flow, ultrasonic wave propagates with a wavelength (λ) much shorter than the bubble radius d_b, i.e. $kd_b \gg 1$, the effect of adsorption/diffraction can be ignored. Under such a condition, the bubbles will act as many acoustic opacities and the mixture can be referred to as strongly inhomogeneous medium [8]. In order to satisfy $kd_b \gg 1$, the radius of bubble should be much larger than 0.12 mm for ultrasound frequency of 2 MHz. As reported by Supardan et al. [13], our system produced mean bubble diameters of 6.1 and 5.8 mm for air–water and air–glycerol 10 wt%, respectively, allowing the adsorption/diffraction effects to be neglected. The ultrasonic measurement was conducted at 75 cm above the gas distributor. In the present experiments, three ultrasound path lengths (L) of 12, 15, and 17 cm were used. A more detail of this experiment can be found elsewhere [14].

To determine the value of X_G of Eq. (2), the attenuation with known gas holdup is plotted against gas holdup-path length ($\varepsilon_G L$). In the experiments, the local gas holdup was estimated using manometer method. Fig. 2 shows the relationship between the attenuation and the gas holdup-path length in air–water and air–glycerol 10 wt% systems for the whole experimental condition. The trend in result is in line with the trend shown by Eqs. (2) and (3) where the attenuation increases with the increase of gas holdup. As the gas holdup increases, the bubble concentration also increases to cause rapid attenuation of the ultrasound. Fig. 2 also shows that the attenuation (I/I_0) in the dispersed system of air–10 wt% glycerol is smaller than that in the air–water system. The possible reasons for this phenomenon are: the denser medium has more mass per volume; it needs more energy to make more mass vibrate. As expected, the more energy is consumed, the more the decrease in the attenuation will occur. The value of X_G can be determined from the gradient of line in Fig. 2. The X_G values were 2.9 and 3.5 for the dispersed system of air–water and air–glycerol 10 wt%, respectively. It is observed that the relationships between the attenuation and gas holdup-path length for two systems used become linear and validate Eq. (2). However, the deviation slightly increased with increasing gas holdup especially for air–glycerol 10 wt%. Following these results, UCT experiments must be conducted at lower gas velocity to maintain high accuracy of ultrasound results from present experimental setup. Then, the attenuation data of ultrasound can be used in the tomography process for determining the cross-sectional gas holdup distribution in the column.

Table 1
Physical properties of water and glycerol 10 wt% solution

	Density (kg/m^3)	Viscosity (mPa s)	Surface tension (mN/m)
Water	998	1.01	72.1
Glycerol 10 wt%	1019	1.31	69.2

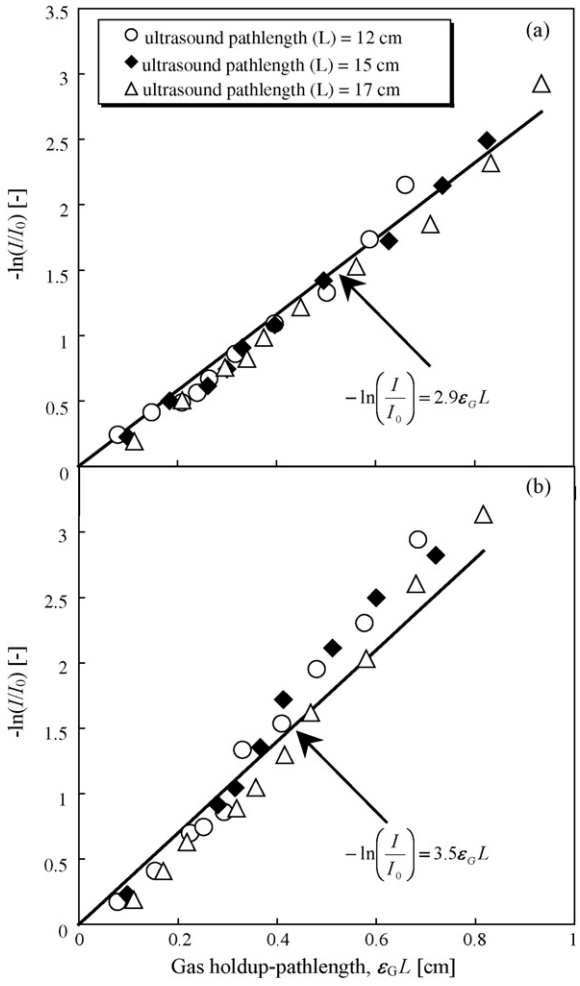

Fig. 2. Relationship between attenuation of ultrasound and gas holdup-path length ($\varepsilon_G L$) for (a) air–water and (b) air–glycerol 10 wt% dispersed system.

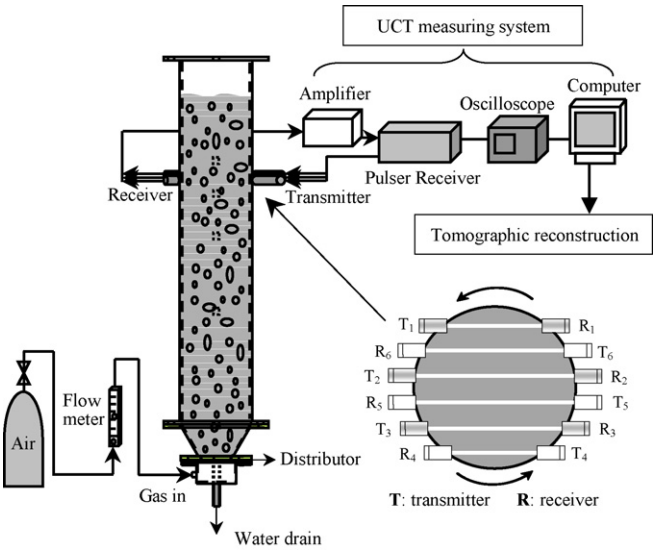

Fig. 3. UCT experimental setup.

2.2. UCT experiments in cylindrical bubble column

Fig. 3 displays in detail the UCT experimental apparatus used in this study. The experiments were performed in a column of 16 cm in diameter and 200 cm in height, made of methylmethaacrylate. The gas distributor is located at the bottom of the conical section and consists of two concentric tubes whose diameters are 3.76 and 1.3 cm in the outer and the inner, respectively. The gas bubbles are dispersed into the column through a perforated plate with six holes of 0.1 cm inner diameter. In all experiments, liquid phases are tap water and aqueous glycerol 10 wt% solution and the gas phase is air. The liquid phase is in batch mode. The static liquid level is about 130 cm.

The UCT measurement used here is the same one as the ultrasound measurement used in the rectangular column experiments described in the previous section. To measure the cross-sectional distribution in the cylindrical bubble column, three parallel transducers array is arranged non-symmetrically and used to perform the tomographic data acquisition. The data of the attenuation energy (I/I_0) acquired in 5 min for every projection path are averaged to obtain the time-average projection data. The transducer array is rotated 20° each, and then the same measurement is repeated until all the projections from nine directions with six paths each are completed. In the tomography reconstruction, the experimental data of 9×6 was increased to 36×11 matrix of integral measurements data using Lagrange interpolation method to obtain better UCT result. As reported by Utomo et al. [11], the accuracy of the reconstructed results is not reduced by using the interpolated data. The corresponding spatial resolution was 5% of column diameter. Warsito et al. [10] explained a more detail of the similar UCT measurements. The measurement was performed at the position above the gas distributor (H) of 30, 55 and 80 cm, respectively. All experiments were performed at the ambient temperature (25 °C) and the atmospheric pressure. The bed expansion method is used to measure the overall gas holdup in the column as an independent technique to validate the accuracy of the UCT results.

2.3. UCT reconstruction procedure

When a slice of the ultrasonic beam penetrates through a two-phase medium, the energy intensity (attenuation) becomes a line integral of the gas holdup along the penetrating path $L_{s,\theta}$, i.e.:

$$p(s,\theta) = \int_{L_{s,\theta}} f(x,y)\,\mathrm{d}l = \overline{\varepsilon_G(s,\theta)} L_{s,\theta} \tag{4}$$

Here s is the distance from the center of the column to the measurement (projection) line and θ is the projection angle. $f(x, y)$ is the probability density function of the gas bubbles in the two-phase medium. The desired function can be obtained using reconstruction procedure such as Fourier transform based on the well-known FBP reconstruction technique.

To improve the accuracy of the reconstruction, the iterative procedure is applied to FBP reconstruction technique. Iterative procedure can be used to overcome the weakness of FBP in noise limitation. Moreover, noise is always contained in the measurement data with varying in magnitude; hence, the robustness of a reconstruction procedure with respect to noise is crucial. The procedure is done as follows [11]:

$$f^{(i+1)} = f^{(i)} + \delta\xi(\Delta p^{(i)}(s,\theta)) \tag{5}$$

where f is the n-dimensional digitized image vector, δ a gain factor, and $\xi(\Delta p^{(i)}(s,\theta))$ denotes the FBP operation on $\Delta p^{(i)}(s, \theta)$. The ith iteration error of the calculated projection is defined as

$$\Delta p^{(i)}(s,\theta) = p(s,\theta) - \sum_{k=1}^{n} \omega_k(s,\theta) f_k^{(i)} \tag{6}$$

where $\omega_k(s,\theta)$ is the element of the projection matrix W, i.e. the intersection area between the pixel kth and the ultrasonic beam strip on the direction θ and distance s from the origin. The IFBP result is obtained by minimizing the iteration error of Eq. (6). The reconstruction procedure used is also the same one as the procedure used by Reinecke et al. [15]. The superiority of IFBP results compared to FBP results in prediction of gas holdup will be presented later.

3. Results and discussion

3.1. Gas holdup from UCT

Fig. 4 shows the typical time-averaged radial distribution of the gas holdup of air–water system in the bubble column at different superficial gas velocities, 0.5, 1.0, 1.25 and 1.5 cm/s, respectively. A gradual variation in the darkness indicates the change in the gas holdup value. From the color scale of the tomogram, it can be seen that the gas holdup profiles change from a flatter distribution to a parabolic one, with increase in the superficial gas velocity. The gas holdup distribution exhibits an asymmetric radial distribution, with higher gas holdup around the column center and lower gas holdup near the column wall. It must be noticed that the highest value of gas holdup is not exactly at the center of the column. The trend findings are consistent

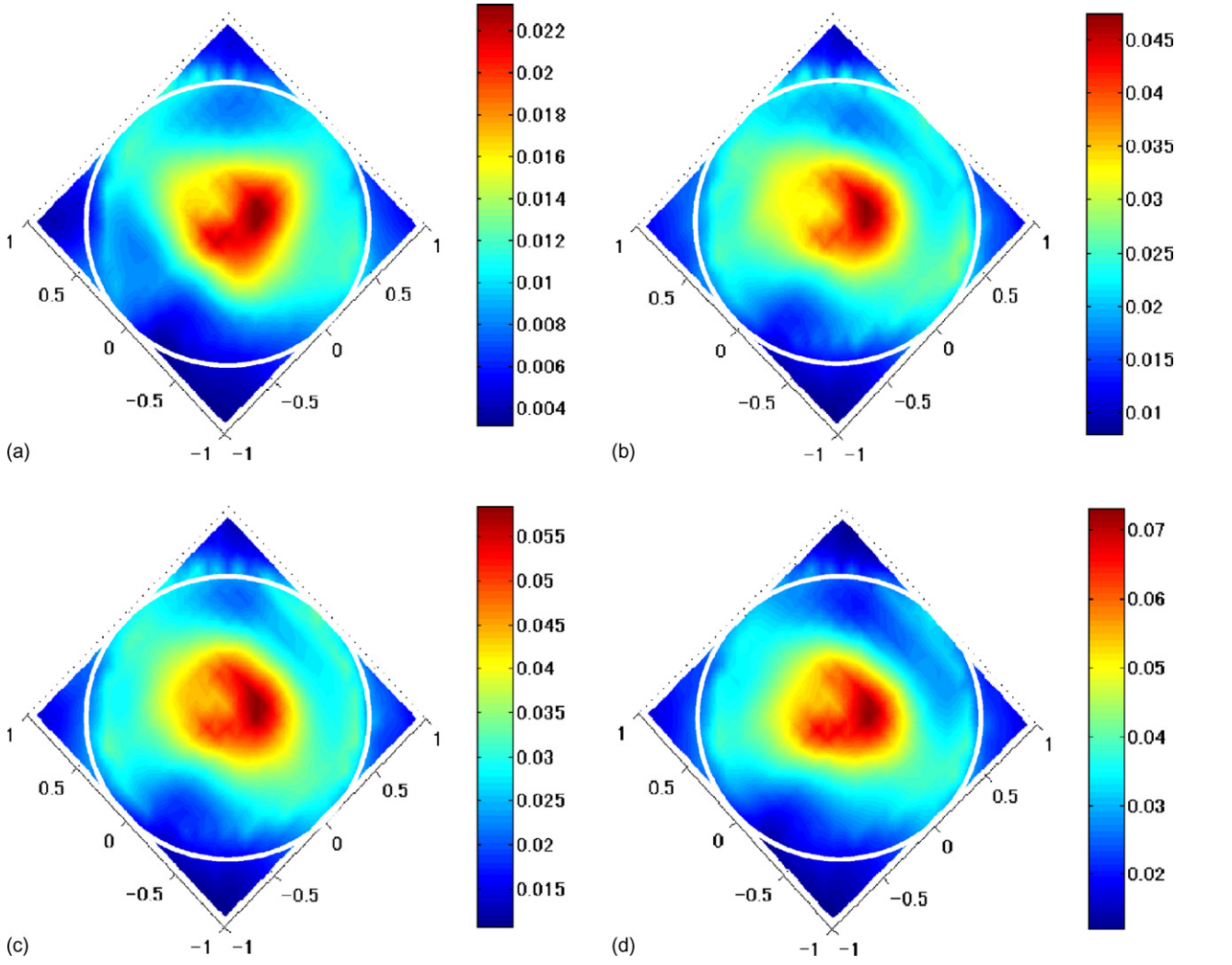

Fig. 4. Time-averaged gas holdup distributions of air–water system at superficial gas velocities of (a) 0.5 cm/s, (b) 1.0 cm/s, (c) 1.25 cm/s and (d) 1.5 cm/s (H = 55 cm).

with that measured using other measuring techniques such as ECT [16] and optical fiber probe [17]. A slight doughnut-shape distribution with a lower gas concentration at the center of the column was observed. The doughnut-shape distribution might be due to the spiral motion of the gas bubbles at low gas velocities. UCT results show that there are no significant changes in the gas holdup distribution with an increase in the UCT measurement position.

In an attempt to check the accuracy of UCT results, a tomographic reconstruction procedure based on IFBP technique has been used to calculate the area-averaged gas holdup distribution. The azimuth and radial averaging was applied to the UCT tomograms. Integration of these profiles over the column cross-section has yielded area-averaged results. As can be seen in Fig. 5, the average gas holdup increases along with the height of UCT measurement position. This trend is in agreement with the result observed by other measuring techniques such as γ-ray densitometer [4,18] and ECT [19]. The reasonable explanation is that the break-up probability of bubbles increases and the coalescence of bubbles decreases with an increase in the system pressure relative to the ambient pressure, which leads to an increase of the holdup with small bubbles. It can also be concluded that the bubbles have not yet developed well in the lower region and are still growing while rising into the upper region.

Fig. 5 also shows the comparison of gas holdup by UCT and that by bed expansion method. It has shown that the average gas holdup measured at the position equal to 80 cm above the distributor or about five times column diameter, is in close agreement with the overall gas holdup in the column.

Kemoun et al. [3] also reported that the cross-sectional gas holdup measured at the height above the distributor higher than four to five column diameters agrees well with the overall gas holdup in the column. The gas holdup results at the measurement position of 80 cm above the distributor has then been chosen to compare the performances of FBP and IFBP reconstruction. Table 2 shows the comparison of the gas holdups by FBP and IFBP results with the gas holdup by bed expansion method. The IFBP was superior in terms of its accuracy to FBP.

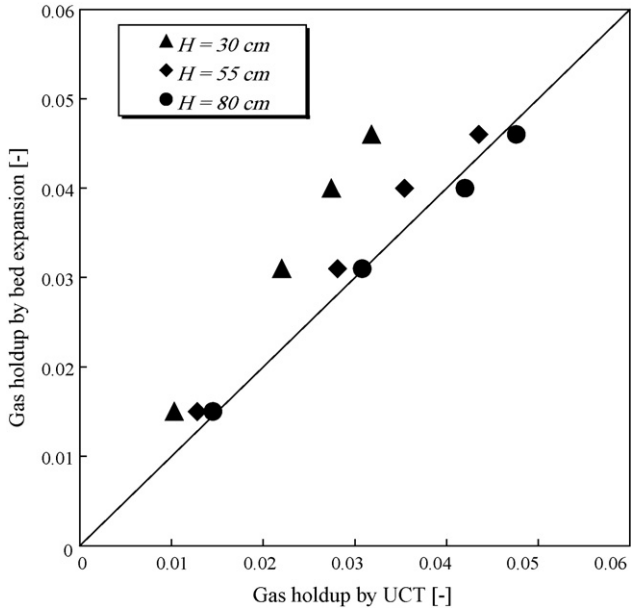

Fig. 5. Effect of UCT measurement position and comparison of UCT method with the bed expansion method for air–water system.

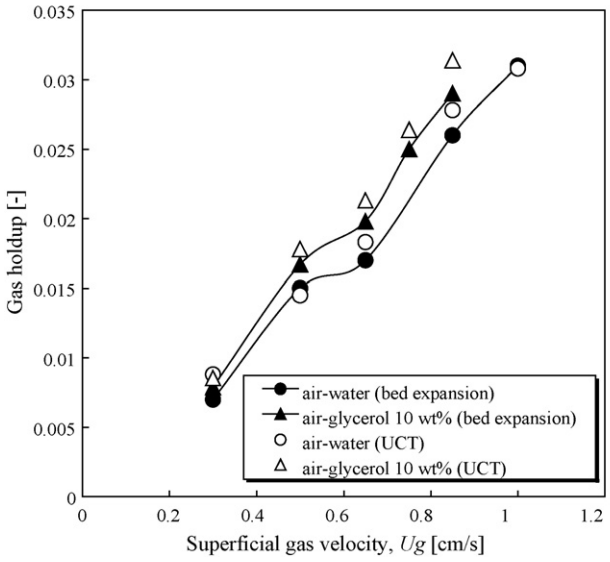

Fig. 6. Cross-sectional average gas holdup as a function of superficial gas velocity ($H = 80$ cm).

As expected, the gas holdup increases with the increase in the gas velocity. This is shown in Fig. 6 for the air–water and air–10 wt% glycerol solution systems. At the same superficial gas velocity, higher gas holdup was observed in the air–glycerol solution than in the air–water. The fundamental reason for this trend of results can be attributed to difference in the physical properties of the system such as surface tension, density and viscosity. The smaller surface tension and higher density of 10 wt% glycerol solution compared with those of tap water leads to larger gas holdup. It can be explained in terms of the bubble terminal velocity. Based on the wave theory, the terminal velocity of bubble can be expressed as [20]:

$$V_\infty \approx \sqrt{\frac{\sigma}{r_e \rho} + g r_e} \tag{7}$$

Eq. (7) shows that the smaller surface tension and higher density results in smaller bubble terminal velocity and consequently, larger gas holdup. In addition, the smaller surface tension might enhance the break-up of large unstable bubbles to smaller bubbles. Meanwhile, Eissa and Schügerl [21] previously reported that viscosity plays a dual role to provide gas holdup. They observed that low viscosity ($\mu < 3$ mPa s) provided an increase in gas holdup, and then, a moderate gas viscosity ($\mu = 3$–11 mPa s) provided a decrease in gas holdup. An almost constant gas holdup is provided at higher viscosity ($\mu > 11$ mPa s). This trend was also reported by other studies [22,23]. The larger drag forces reduce the bubble rise velocity and an increase in gas holdup is found at a low viscosity. At the same time, these forces are not strong enough to promote the coalescence. At a higher viscosity, the tendency to coalesce and polydispersity prevails over the drag reduction and the uniformity is broken by big bubbles. This supposition is in line with the experimental results. Since the viscosity of glycerol 10 wt% used is smaller than 3 mPa s, a higher gas holdup was observed in the air–glycerol solution than in the air–water system.

Fig. 6 also shows the corresponding gas holdup obtained by bed expansion method. It can be concluded that the UCT results give reasonable estimate of local gas holdup investigated in this study. It was found that the average error between UCT and bed expansion method is about 7%. These errors could be caused by the limitation in the strength of the current ultrasonic wave used. Another possible error sources were due to the linearity approximations of Eq. (2).

Table 3 compares the present result of average gas holdup measured by UCT with the data obtained from literature of air–tap water system. The associated experimental condition is also presented. Compared to Kemoun's result, the present one shows a reasonable result but significantly deviated from the Shollenberger's study. As the gas holdup increases with increasing column diameter, higher gas holdup should then have been expected in Shollenberger's study as compared to the present one. The possible reasons were the differences in the measurement position and the type of distributor used as listed in Table 3.

Table 2
Comparison of UCT result with those by FBP and IFBP

Superficial gas velocity (cm/s)	Gas holdup		
	FBP	IFBP	Bed expansion
0.5	0.005	0.014	0.015
1.0	0.014	0.029	0.031
1.25	0.022	0.042	0.040
1.50	0.029	0.048	0.046

* Air–water system; $H = 80$ cm.

Table 3
Comparison of UCT result with literature data for air–water system

	Column diameter (cm)	U_g (cm/s)	Gas holdup	Distributor type	H (cm)
Shollenberger et al. [5]	19	1.47	0.024	Bubble cap	57
Kemoun et al. [3]	16.2	2	0.069	Perforated	92
Present study (UCT)	16	1.5	0.048	Perforated	80

3.2. Analysis of the system with attached baffle

Gas holdup distribution in a bubble column with an attached baffle is also investigated. At the position of 50 cm above the distributor a baffle is attached to block a half or three-fourth portion of the cross-section. In order to observe the evolution of gas holdup, the UCT measurements were conducted at three points of 30, 55 and 80 cm above the gas distributor. Fig. 7 represents the description of the system and the image of the baffle used.

Fig. 8 shows the time-averaged gas holdup distribution predicted by UCT in a bubble column with an attached baffle. Again, it is clear that the gas holdup distribution exhibits asymmetric radial distributions for two kinds of baffles used. There is no apparent change in the gas holdup distribution with an increase in the superficial gas velocity. As presented before, the higher gas holdup around the column center and a lower gas holdup near the column wall are observed in the column without a baffle. On the contrary, it tends to be higher near one part of the column wall in the column with an attached baffle at the measurement position of 5 cm above the attached baffle. The difference of gas holdup distribution for two kinds of baffles can be observed clearly.

The gas holdup distribution in the column with a half block baffle at three different measurement positions is shown in Fig. 9. A photograph is also presented as a comparison. Both UCT and photographic method show the same trend. At $H = 30$ cm, the almost similar gas holdup distribution as that in the column without attached baffle is observed. The effect of the baffle presence on the gas holdup distribution is clearly observed at $H = 55$ cm (5 cm above the attached baffle). The gas holdup tends to be higher near one side of the column. The effect of baffle diminishes as the UCT measurement position becomes higher. As can be seen in Fig. 9, the gas holdup distribution starts to be the same as that in the column without a baffle at $H = 80$ cm.

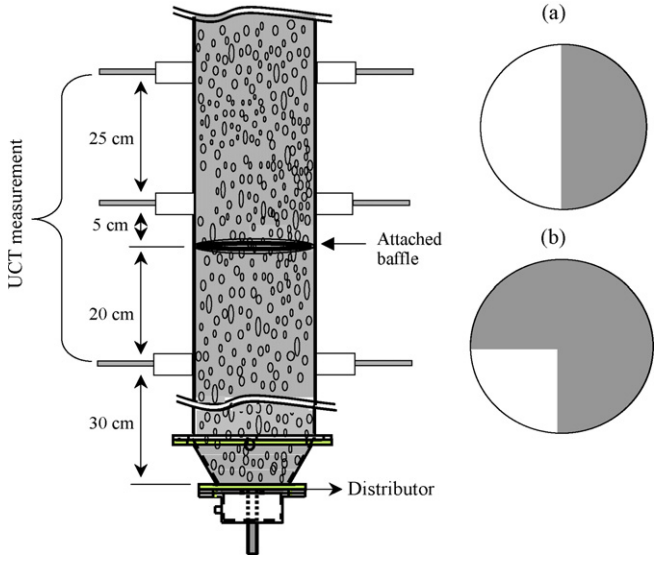

Fig. 7. Description of bubble column with an attached baffle and baffle used (a) half blocked and (b) three-fourth blocked.

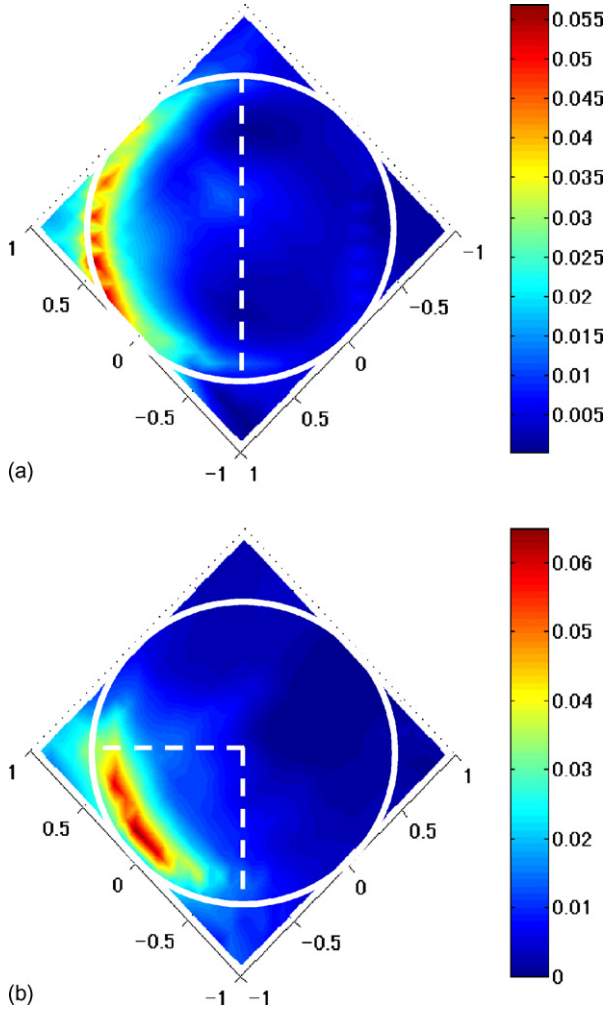

Fig. 8. Gas holdup distribution in bubble column with an attached baffles for superficial gas velocity 1.25 cm/s at $H = 55$ cm: (a) half blocked and (b) three-fourth blocked.

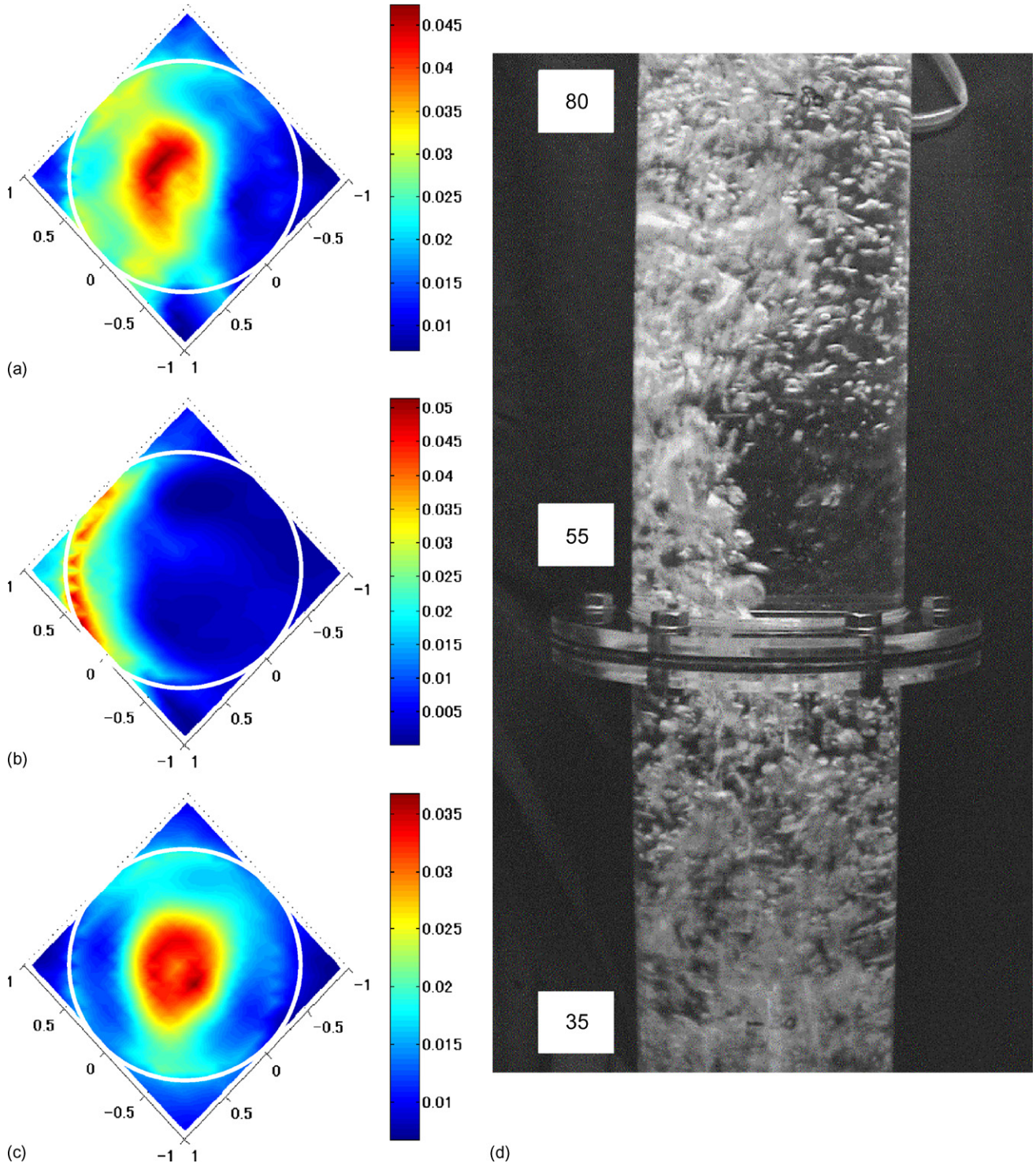

Fig. 9. Gas holdup distribution in bubble column with an attached baffle of half blocked for superficial gas velocity 1.0 cm/s: (a) $H = 80$ cm, (b) $H = 55$ cm, (c) $H = 30$ cm and (d) the associated photographic result.

4. Conclusion

In the present study, although the time-averaged cross-sectional distributions were investigated, UCT has been successful to show the general trends of the gas holdup of two-phase system in a bubble column. The gas holdup distributions in a bubble column have become clear by non-invasive technique of UCT. The gas holdups determined by the UCT are in a good agreement with the experimental results obtained by the bed expansion method. It is confirmed that a higher gas holdup in the air–glycerol solution than in the air–water system. The difference in gas holdup distribution due to the presence of baffle can also be observed by using UCT. The present results show the potential to implement UCT for analyzing complex system

such as an oscillatory baffled column that is also widely applied in chemical processes.

References

[1] L.G. Neal, S.G. Bankoff, A high resolution resistivity probe for determination of local void properties in gas–liquid flow, AIChE J. 9 (1964) 490–494.

[2] E. Fransolet, M. Crine, G. L'Homme, D. Toye, P. Marchot, Analysis of electrical resistance tomography measurements obtained on a bubble column, Meas. Sci. Technol. 12 (2001) 1055–1060.

[3] A. Kemoun, B.C. Ong, P. Gupta, M.H. Al-Dahhan, M.P. Dudukovic, Gas holdup in bubble columns at elevated pressure via computed tomography, Int. J. Multiphase Flow 27 (2001) 929–946.

[4] S.B. Kumar, D. Moslemian, M.P. Dudukovic, Gas holdup measurements in bubble columns using computed tomography, AIChE J. 43 (1997) 1414–1425.

[5] K.A. Shollenberger, J.R. Torczynski, D.R. Adkins, T.J. O'Hern, N.B. Jackson, Gamma-densitometry tomography of gas holdup spatial distribution in industrial-scale bubble columns, Chem. Eng. Sci. 52 (1997) 2037–2048.

[6] U.P. Veera, J.B. Joshi, Measurements of gas holdup profiles by gamma ray tomography, Trans. Inst. Chem. Eng. 77 (1999) 303–317.

[7] B.S. Hoyle, L.A. Xu, Ultrasonic sensors, in: R.A. Williams, M.S. Beck (Eds.), Process Tomography Principles, Techniques and Applications, Butterworth Heinemann, Oxford, 1995, pp. 175–208.

[8] L. Xu, Y. Han, L.A. Xu, J. Yang, Application of ultrasonic tomography to monitoring gas/liquid flow, Chem. Eng. Sci. 52 (1997) 2171–2183.

[9] W. Li, B.S. Hoyle, Ultrasonic process tomography using multiple active sensors for maximum real-time performance, Chem. Eng. Sci. 52 (1997) 2161–2170.

[10] Warsito, M. Ohkawa, N. Kawata, S. Uchida, Cross-sectional distributions of gas and solid holdups in slurry bubble column investigated by ultrasonic computed tomography, Chem. Eng. Sci. 54 (1999) 4711–4728.

[11] M.B. Utomo, Warsito, T. Sakai, S. Uchida, Analysis of distributions of gas and TiO_2 particles in slurry bubble column using ultrasonic computed tomography, Chem. Eng. Sci. 56 (2001) 6073–6079.

[12] V. Stolojanu, A. Prakash, Hydrodynamic measurements in a slurry bubble column using ultrasonic technique, Chem. Eng. Sci. 52 (1997) 4225–4230.

[13] M.D. Supardan, Y. Masuda, A. Maezawa, S. Uchida, Measurement of interfacial area using ultrasonic technique in a two-dimensional bubble column, J. Chem. Eng. Jpn., submitted for publication.

[14] M.D. Supardan, Y. Masuda, A. Maezawa, S. Uchida, Local gas holdup and mass transfer in a bubble column using and ultrasonic technique and a neural network, J. Chem. Eng. Jpn. 37 (2004) 927–932.

[15] N. Reinecke, G. Petritsch, D. Schmitz, D. Mewes, Tomographic measurement techniques—visualization of multiphase flows, Chem. Eng. Technol. 21 (1998) 7–18.

[16] W. Warsito, L.S. Fan, ECT imaging of three-phase fluidized bed based on three-phase capacitance model, Chem. Eng. Sci. 58 (2003) 823–832.

[17] J.-M. Schweitzer, J. Bayle, T. Gauthier, Local gas-up measurements in fluidized bed and slurry bubble column, Chem. Eng. Sci. 56 (2001) 1103–1110.

[18] H. Jin, S. Yang, G. He, Z. Guo, Z. Tong, An experimental study of holdups in large-scale *p*-xylene oxidation reactors using the γ-ray attenuation approach, Chem. Eng. Sci. 60 (2005) 5955–5961.

[19] W. Warsito, L.S. Fan, Measurement of real-time flow structures in gas–liquid and gas–liquid–solid flow systems using electrical capacitance tomography (ECT), Chem. Eng. Sci. 56 (2001) 6455–6462.

[20] H.D. Mendelson, The prediction of bubble terminal velocities from wave theory, AIChE J. 13 (1967) 250–252.

[21] S.H. Eissa, K. Schügerl, Holdup and backmixing investigation in cocurrent and countercurrent bubble columns, Chem. Eng. Sci. 30 (1975) 1251–1256.

[22] J.J. Heijnen, K. van Riet, Mass transfer, mixing and heat transfer phenomena in low viscosity bubble column reactor, Chem. Eng. J. 28 (1984) B21–B42.

[23] M.C. Ruzicka, J. Drahos, P.C. Mena, J.A. Teixeira, Effect of viscosity on homogeneous–heterogeneous flow regime transition in bubble columns, Chem. Eng. J. 96 (2003) 15–22.